Proceedings of the 1999 IEEE
International Conference on Control Applications
Kohala Coast-Island of Hawai'i, Hawai'i, USA • August 22-27, 1999

Adaptive Nonlinear Control of Repulsive Maglev Suspension Systems

Chao-Ming Huang Min-Shin Chen Jia-Yush Yen
Ph.D. Candidate Professor Professor
Department of Mechanical Engineering,
National Taiwan University,
Taipei, Taiwan 10617, R.O.C.

Abstract

Magnetic levitation systems have recently become the focus of many research interests not only because they are most suitable for high precision engineering applications but also due to the fact that they represent a difficult challenge to control engineers. As a result, most previous studies have focused on the control stabilization problem. In this paper, we address the issue of performance with respect to uncertainty in order to achieve a desired rigidity. The proposed controller is an adaptive backstepping controller. The adaptive backstepping controller provides system stability under model uncertainty, and achieves the desired servo performance. The experiments show that the proposed control achieves a superior behavior than other control.

1. Introduction

With the development of the industry technology, numerous motion control devices and advanced fabrication equipment's have been designed to meet the high-precision positioning demand. Due to the non-contact characteristics, the suspension system based on maglev technology plays an important role in the positioning system design. A maglev system can be classified, based on the levitation forces, as an attractive system or a repulsive system. Most of the maglev systems discussed in the literature are attractive systems, where attractive forces are applied between the moving carriage and fixed guide rails [1]~[5]. On the other hand, the repulsive maglev systems use repulsive forces to push the moving carriage above the fixed guide rails [1], [6], [7], [8].

Maglev technology can also be classified into the passive maglev which uses two permanent magnets with the same poles facing each other to generate repulsive force, and the active maglev which uses a permanent magnet levitated above a dc electromagnet. The experimental device used in this paper (Figure 1, 2) is a repulsive maglev suspension system; however, it is neither active nor passive. Our design is to compound both active and passive maglev technique designs.

When using active maglev only, one must apply current to dc electromagnets all the time to make carriage fly, but this will overheat the levitation coils of electromagnets, liquefy the lacquer protection, and lead to short-circuit of the coils. Our system puts the active maglev and the passive maglev designs together, the combined system can work without these problems. That is because the passive device will provide an equivalent bias current to levitate the carriage and prevent the system from the risk mentioned above. In our system, active component plays the role of improving robustness of the passive component when necessary. The main objective in this paper is to control the attitude of carriage to a desired operating point with respect to the two degrees of freedom (D.O.F.) X and θ only (Figure 2). The other three D.O.F. ϕ, ψ, and Z are neglected because their dynamics are the stable zero dynamics of the system and will approach zero asymptotically [7]. In an up-coming paper, we will use the active maglev components to complete the control of the whole five D.O.F. in our system.

The maglev suspension system is a nonlinear system with complicated model. It is hard to design classical controllers because of its strongly coupled nature. In this paper, a multi-input-multi-output adaptive backstepping control is derived and implemented. The results show that the adaptive backstepping controller for the maglev system is better than the H-infinitive control based on a linear system model in [7] or the adaptive control without backstepping in [8].

In this paper, a precise model of the maglev suspension system will be derived first, and we will analyze the sources of uncertainty parameters. Then the adaptive backstepping control will be applied to the system experimentally. Results will be shown and compared with others in [7], [8].

2. Experimental Device and Model

2.1 Mechanical Dynamics

Basically, the maglev suspension system is a five-input-five-output system. Here, the five outputs are X, θ, ϕ, ψ, and Z (Figure 2). The five inputs are currents I_{stab1}, I_{stab2}, I_{lev1}, I_{lev2}, I_{lev3} which will be applied into levitation tracks in Figure 2. The relationships between each track and applied currents are listed in Table 1. The dynamics of the maglev system can be divided into a stable part and an unstable part. The stable part consists of the dynamics of ϕ, ψ, and Z, which are stable by design. Therefore, in this paper, we will focus only on the unstable part, the dynamics of X and θ, the other three states, ϕ, ψ, and Z are left without control. As a result, the active component of levitator can be turned off in this application and the system is reduced to two-input-two-output, which is a subsystem of the whole maglev system. In future researches, we will extend the control problem to five-input-five-output and the active component of levitator will be turned on in that case. But this must be done under the assumption that the unstable part of the maglev system is well-controlled, which is the objective of this paper.

In the X and θ dynamics, the track magnets and carriage magnets in passive levitator (Figure 3) lift the carriage; however, this produces destabilizing forces F_{AM}, F_{BM}, F_{CM}, and F_{DM}, which will destabilize X, θ (Figure 4). By applying currents I_{stab1}, I_{stab2} to stabilizer coils, we can obtain stabilizing forces F_{AS}, F_{BS}, F_{CS}, and F_{DS} to make X, θ stable. A model of maglev suspension system can be obtained, using Newton-Euler equations of motion for a body that moves in space (Figure 4), with the following form:

$$\ddot{\theta} = \frac{1}{I_z}\{(-a_1 + b_1\theta)(F_{AS} + F_{BS} + F_{AM} + F_{BM}) + (a_2 + b_2\theta)(F_{CS} + F_{DS} + F_{CM} + F_{DM})\} \quad (1)$$

$$\ddot{X} = \frac{1}{M}(F_{AS} + F_{BS} + F_{CS} + F_{DS} + F_{AM} + F_{BM} + F_{CM} + F_{DM}) \quad (2)$$

where

$$F_{AS} = N_{SA}\frac{\mu_0 I_{stab1}}{2\pi}\left\{\frac{-(d+\delta A_X)^2\Omega_{ZA}}{[(d+\delta A_X)^2]^2}+\frac{-(-d+\delta A_X)^2\Omega_{ZA}}{[(-d+\delta A_X)^2]^2}\right\} \quad (3)$$

$$F_{BS} = N_{SB}\frac{\mu_0 I_{stab1}}{2\pi}\left\{\frac{-(d+\delta B_X)^2\Omega_{ZB}}{[(d+\delta B_X)^2]^2}+\frac{-(-d+\delta B_X)^2\Omega_{ZB}}{[(-d+\delta B_X)^2]^2}\right\} \quad (4)$$

$$F_{CS} = N_{SC}\frac{\mu_0 I_{stab2}}{2\pi}\left\{\frac{-(d+\delta C_X)^2\Omega_{ZC}}{[(d+\delta C_X)^2]^2}+\frac{-(-d+\delta C_X)^2\Omega_{ZC}}{[(-d+\delta C_X)^2]^2}\right\} \quad (5)$$

$$F_{DS} = N_{SD}\frac{\mu_0 I_{stab2}}{2\pi}\left\{\frac{-(d+\delta D_X)^2\Omega_{ZD}}{[(d+\delta D_X)^2]^2}+\frac{-(-d+\delta D_X)^2\Omega_{ZD}}{[(-d+\delta D_X)^2]^2}\right\} \quad (6)$$

$$F_{AM} = \frac{\mu_0 I_{mA}}{2\pi}\left\{-\frac{\left[e_M^2-(c_M+\delta A_X)^2\right]\Omega_{ZA}}{\left[(c_M+\delta A_X)^2+e_M^2\right]^2}+\frac{\left[e_M^2-(-c_M+\delta A_X)^2\right]\Omega_{ZA}}{\left[(-c_M+\delta A_X)^2+e_M^2\right]^2}\right\} \quad (7)$$

$$F_{BM} = \frac{\mu_0 I_{mB}}{2\pi}\left\{-\frac{\left[e_M^2-(c_M+\delta B_X)^2\right]\Omega_{ZB}}{\left[(c_M+\delta B_X)^2+e_M^2\right]^2}+\frac{\left[e_M^2-(-c_M+\delta B_X)^2\right]\Omega_{ZB}}{\left[(-c_M+\delta B_X)^2+e_M^2\right]^2}\right\} \quad (8)$$

$$F_{CM} = \frac{\mu_0 I_{mC}}{2\pi}\left\{-\frac{\left[e_M^2-(c_M+\delta C_X)^2\right]\Omega_{ZC}}{\left[(c_M+\delta C_X)^2+e_M^2\right]^2}+\frac{\left[e_M^2-(-c_M+\delta C_X)^2\right]\Omega_{ZC}}{\left[(-c_M+\delta C_X)^2+e_M^2\right]^2}\right\} \quad (9)$$

$$F_{DM} = \frac{\mu_0 I_{mD}}{2\pi}\left\{-\frac{\left[e_M^2-(c_M+\delta D_X)^2\right]\Omega_{ZD}}{\left[(c_M+\delta D_X)^2+e_M^2\right]^2}+\frac{\left[e_M^2-(-c_M+\delta D_X)^2\right]\Omega_{ZD}}{\left[(-c_M+\delta D_X)^2+e_M^2\right]^2}\right\} \quad (10)$$

$$\delta A_X = -a_1\theta + X \quad (11)$$

$$\delta B_X = -a_1\theta + X \quad (12)$$

$$\delta C_X = a_2\theta + X \quad (13)$$

$$\delta D_X = a_2\theta + X \quad (14)$$

All model parameters are listed in Table 2 and Figure 4. Readers can refer to [7], [8] for more details about this magnetic force model. Finally, the general system can be rearranged in a control-affine form:

$$\ddot{x}_1 = F_1(x_1,x_2)+G_{11}(x_1,x_2)I_{stab1}+G_{12}(x_1,x_2)I_{stab2} \quad (15)$$

$$\ddot{x}_2 = F_2(x_1,x_2)+G_{21}(x_1,x_2)I_{stab1}+G_{22}(x_1,x_2)I_{stab2} \quad (16)$$

where $x_1=\theta$, $x_2=X$, and F_1, F_2, G_{11}, G_{12}, G_{21}, G_{22} are functions of x_1, x_2.

2.2 Actuator Dynamics

The actuator dynamics of the maglev suspension system are:

$$\dot{I}_{stab1} = -\frac{R_1}{L_1}I_{stab1}+\frac{K_{D1}}{L_1}u_1 = \lambda_1 I_{stab1}+\kappa_1 u_1 \quad (17)$$

$$\dot{I}_{stab2} = -\frac{R_2}{L_2}I_{stab2}+\frac{K_{D2}}{L_2}U_2 = \lambda_2 I_{stab2}+\kappa_2 u_2 \quad (18)$$

where R_1, R_2 are resistor of maglev system coils, L_1, L_2 are inductor of maglev system coils, and K_{D1}, K_{D2} are gains of power amplifiers. u_1, u_2 are the real control input voltages to the system. By combining both mechanical dynamics and actuator dynamics, the model of maglev suspension system can be derived.

3. Model Uncertainties Analysis

In the previous section, we obtain the mathematical model of the maglev suspension system. In this section, we will discuss which system parameters in the maglev system are to be treated as uncertainties. Parameters, a_1, a_2, b_1, b_2, d, c_M, and e_M in (1)~(14), which are dimensions of the system, can be accurately measured. N_{SA}, N_{SB}, N_{SC}, and N_{SD} in (3)~(6) are the turns of stabilizer coils, whose precise knowledge are known. Mass and inertia of carriage, M and I_Z, are parameters difficult to obtain due to their complex structures and nonuiformity of materials. Other parameters Ω_{ZA}, Ω_{ZB}, Ω_{ZC}, Ω_{ZD}, I_{mA}, I_{mB}, I_{mC} and I_{mD}, which are unmeasurable magnetic properties of the system and will be the major source of uncertain parameters.

Collecting the uncertain parameters in (1)~(14), the system equation can be re-grouped as

$$\ddot{x}_1 = \alpha_1^T f_1(x_1,x_2)+\beta_{11}g_{11}(x_1,x_2)I_{stab1}+\beta_{12}g_{12}(x_1,x_2)I_{stab2} \quad (19)$$

$$\ddot{x}_2 = \alpha_2^T f_2(x_1,x_2)+\beta_{21}g_{21}(x_1,x_2)I_{stab1}+\beta_{22}g_{22}(x_1,x_2)I_{stab2} \quad (20)$$

where $\alpha_1\in R^2$, $\alpha_2\in R^2$, $\beta_{11}\in R^1$, $\beta_{12}\in R^1$, $\beta_{21}\in R^1$, $\beta_{22}\in R^1$ are treated as unknown system parameters, and $f_1\in R^2$, $f_2\in R^2$, $g_{11}\in R^1$, $g_{12}\in R^1$, $g_{21}\in R^1$, $g_{22}\in R^1$ are known functions of the system states. They are all listed in the appendix. Coupling the actuator dynamics (17), (18) with the parameterized system (19), (20), we obtain the overall system equations:

$$\begin{cases}\dot{x}_1 = x_3\\ \dot{x}_2 = x_4\\ \dot{x}_3 = \alpha_1^T f_1(x_1,x_2)+\beta_{11}g_{11}(x_1,x_2)I_{stab1}+\beta_{12}g_{12}(x_1,x_2)I_{stab2}\\ \dot{x}_4 = \alpha_2^T f_2(x_1,x_2)+\beta_{21}g_{21}(x_1,x_2)I_{stab1}+\beta_{22}g_{22}(x_1,x_2)I_{stab2}\\ \dot{I}_{stab1} = \lambda_1 I_{stab1}+\kappa_1 u_1\\ \dot{I}_{stab2} = \lambda_2 I_{stab2}+\kappa_2 u_2\end{cases} \quad (21)$$

4. Controller Design

The control objective is to drive the system output x_1 and x_2 to zero asymptotically. First, we introduce a new coordinate system

$$z_1 = x_1 \quad (22)$$

$$z_2 = x_2 \quad (23)$$

$$z_3 = x_3 - v_1(z_1) \quad (24)$$

$$z_4 = x_4 - v_2(z_2) \quad (25)$$

$$z_5 = I_{stab1} - v_3(z_1,z_2,z_3,z_4) \quad (26)$$

$$z_6 = I_{stab2} - v_4(z_1,z_2,z_3,z_4) \quad (27)$$

where

$$v_1(x_1) = -k_1 z_1 \quad (28)$$

$$v_2(x_2) = -k_2 z_2 \quad (29)$$

$$\begin{bmatrix}v_3\\ v_4\end{bmatrix} = \begin{bmatrix}\hat{\beta}_{11}g_{11} & \hat{\beta}_{12}g_{12}\\ \hat{\beta}_{21}g_{21} & \hat{\beta}_{22}g_{22}\end{bmatrix}^{-1}\begin{bmatrix}-\hat{\alpha}_1^T f_1+\frac{\partial v_1(z_1)}{\partial z_1}(z_3+v_1)-k_3 z_3-z_1\\ -\hat{\alpha}_2^T f_2+\frac{\partial v_2(z_2)}{\partial z_2}(z_4+v_2)-k_4 z_4-z_2\end{bmatrix} \quad (30)$$

and $\hat{\alpha}_1$, $\hat{\alpha}_2$, $\hat{\beta}_{11}$, $\hat{\beta}_{12}$, $\hat{\beta}_{21}$, $\hat{\beta}_{22}$ are estimates of α_1, α_2, β_{11}, β_{12}, β_{21}, β_{22} respectively. We can get new dynamical equations as follows

$$\dot{z}_1 = z_3 - k_1 z_1 \quad (31)$$

$$\dot{z}_2 = z_4 - k_2 z_2 \quad (32)$$

$$\begin{bmatrix}\dot{z}_3\\ \dot{z}_4\end{bmatrix} = \begin{bmatrix}-k_3 z_3 - z_1\\ -k_4 z_4 - z_2\end{bmatrix}+\begin{bmatrix}\hat{\beta}_{11}g_{11} & \hat{\beta}_{12}g_{12}\\ \hat{\beta}_{21}g_{21} & \hat{\beta}_{22}g_{22}\end{bmatrix}\begin{bmatrix}z_5\\ z_6\end{bmatrix}+\begin{bmatrix}\tilde{\gamma}_1^T\omega_1\\ \tilde{\gamma}_2^T\omega_2\end{bmatrix} \quad (33)$$

$$\begin{bmatrix}\dot{z}_5\\ \dot{z}_6\end{bmatrix}=\begin{bmatrix}\lambda_1(z_5+v_3)\\ \lambda_2(z_6+v_4)\end{bmatrix}+\begin{bmatrix}\kappa_1 u_1\\ \kappa_2 u_2\end{bmatrix}-\begin{bmatrix}\frac{\partial v_3}{\partial z_3} & \frac{\partial v_3}{\partial z_4}\\ \frac{\partial v_4}{\partial z_3} & \frac{\partial v_4}{\partial z_4}\end{bmatrix}\begin{bmatrix}z_3+v_1\\ z_4+v_2\end{bmatrix}-\begin{bmatrix}\frac{\partial v_3}{\partial \hat{\gamma}_1} & \frac{\partial v_3}{\partial \hat{\gamma}_2}\\ \frac{\partial v_4}{\partial \hat{\gamma}_1} & \frac{\partial v_4}{\partial \hat{\gamma}_2}\end{bmatrix}\begin{bmatrix}\dot{\hat{\gamma}}_1\\ \dot{\hat{\gamma}}_2\end{bmatrix}$$
$$-\begin{bmatrix}\frac{\partial v_3}{\partial z_3} & \frac{\partial v_3}{\partial z_4}\\ \frac{\partial v_4}{\partial z_3} & \frac{\partial v_4}{\partial z_4}\end{bmatrix}\left\{\begin{bmatrix}-k_3z_3-z_1\\ -k_4z_4-z_2\end{bmatrix}+\begin{bmatrix}\hat{\beta}_{11}g_{11} & \hat{\beta}_{12}g_{12}\\ \hat{\beta}_{21}g_{21} & \hat{\beta}_{22}g_{22}\end{bmatrix}\begin{bmatrix}z_5\\ z_6\end{bmatrix}\right\} \quad (34)$$
$$-\begin{bmatrix}\tilde{\gamma}_1^T\frac{\partial v_3}{\partial z_3}\omega_1+\tilde{\gamma}_2^T\frac{\partial v_3}{\partial z_4}\omega_2\\ \tilde{\gamma}_1^T\frac{\partial v_4}{\partial z_3}\omega_1+\tilde{\gamma}_2^T\frac{\partial v_4}{\partial z_4}\omega_2\end{bmatrix}$$

where

$$\gamma_1^T=\{\alpha_1^T \quad \beta_{11} \quad \beta_{12}\},\ \gamma_2^T=\{\alpha_2^T \quad \beta_{21} \quad \beta_{22}\},$$
$$\hat{\gamma}_1^T=\{\hat{\alpha}_1^T \quad \hat{\beta}_{11} \quad \hat{\beta}_{12}\},\ \hat{\gamma}_2^T=\{\hat{\alpha}_2^T \quad \hat{\beta}_{21} \quad \hat{\beta}_{22}\},$$
$$\tilde{\gamma}_1=\gamma_1-\hat{\gamma}_1,\ \tilde{\gamma}_2=\gamma_2-\hat{\gamma}_2,$$
$$\omega_1=\begin{bmatrix}f_1\\ g_{11}\sigma_1\\ g_{12}\sigma_2\end{bmatrix},\quad \omega_2=\begin{bmatrix}f_2\\ g_{21}\sigma_1\\ g_{21}\sigma_2\end{bmatrix},$$
$$\begin{bmatrix}\sigma_1\\ \sigma_2\end{bmatrix}=\begin{bmatrix}\hat{\beta}_{11}g_{11} & \hat{\beta}_{12}g_{12}\\ \hat{\beta}_{21}g_{21} & \hat{\beta}_{22}g_{22}\end{bmatrix}^{-1}\begin{bmatrix}-\hat{\alpha}_1^T f_1+\frac{\partial v_1(z_1)}{\partial z_1}(z_3+v_1)-k_3z_3-z_1\\ -\hat{\alpha}_2^T f_2+\frac{\partial v_2(z_2)}{\partial z_2}(z_4+v_2)-k_4z_4-z_2\end{bmatrix}+\begin{bmatrix}z_5\\ z_6\end{bmatrix}$$

For the above system, we propose the following adaptive backstepping control:

$$\begin{bmatrix}u_1\\ u_3\end{bmatrix}=\begin{bmatrix}\kappa_1 & 0\\ 0 & \kappa_2\end{bmatrix}^{-1}\left\{-\begin{bmatrix}\lambda_1(z_5+v_3)\\ \lambda_2(z_6+v_4)\end{bmatrix}-\begin{bmatrix}k_5z_5\\ k_6z_6\end{bmatrix}-\begin{bmatrix}\rho_1\\ \rho_2\end{bmatrix}\right\} \quad (35a)$$

$$\begin{bmatrix}\rho_1\\ \rho_2\end{bmatrix}=-\begin{bmatrix}\frac{\partial v_3}{\partial z_3} & \frac{\partial v_3}{\partial z_4}\\ \frac{\partial v_4}{\partial z_3} & \frac{\partial v_4}{\partial z_4}\end{bmatrix}\begin{bmatrix}z_3+v_1\\ z_4+v_2\end{bmatrix}-\begin{bmatrix}\frac{\partial v_3}{\partial \hat{\gamma}_1} & \frac{\partial v_3}{\partial \hat{\gamma}_2}\\ \frac{\partial v_4}{\partial \hat{\gamma}_1} & \frac{\partial v_4}{\partial \hat{\gamma}_2}\end{bmatrix}\begin{bmatrix}\dot{\hat{\gamma}}_1\\ \dot{\hat{\gamma}}_2\end{bmatrix}$$
$$-\begin{bmatrix}\frac{\partial v_3}{\partial z_3} & \frac{\partial v_3}{\partial z_4}\\ \frac{\partial v_4}{\partial z_3} & \frac{\partial v_4}{\partial z_4}\end{bmatrix}\left\{\begin{bmatrix}-k_3z_3-z_1\\ -k_4z_4-z_2\end{bmatrix}-\begin{bmatrix}\hat{\beta}_{11}g_{11} & \hat{\beta}_{12}g_{12}\\ \hat{\beta}_{21}g_{21} & \hat{\beta}_{22}g_{22}\end{bmatrix}\begin{bmatrix}z_5\\ z_6\end{bmatrix}\right\} \quad (35b)$$

and the update law

$$\dot{\hat{\gamma}}_1=\Gamma_1\omega_1\left(z_1-\frac{\partial v_3}{\partial z_3}z_5-\frac{\partial v_4}{\partial z_3}z_6\right) \quad (35c)$$

$$\dot{\hat{\gamma}}_2=\Gamma_2\omega_2\left(z_4-\frac{\partial v_3}{\partial z_4}z_5-\frac{\partial v_4}{\partial z_4}z_6\right) \quad (35d)$$

where $\Gamma_1=\Gamma_1^T>0$, $\Gamma_2=\Gamma_2^T>0$ are the adaptation gains. Then the closed-loop dynamics of z_5, z_6 becomes

$$\begin{bmatrix}\dot{z}_5\\ \dot{z}_6\end{bmatrix}=-\begin{bmatrix}k_5z_5\\ k_6z_6\end{bmatrix}-\begin{bmatrix}\hat{\beta}_{11}g_{11} & \hat{\beta}_{12}g_{12}\\ \hat{\beta}_{21}g_{21} & \hat{\beta}_{22}g_{22}\end{bmatrix}^T\begin{bmatrix}z_3\\ z_4\end{bmatrix}-\begin{bmatrix}\tilde{\gamma}_1^T\frac{\partial v_3}{\partial z_3}\omega_1+\tilde{\gamma}_2^T\frac{\partial v_3}{\partial z_4}\omega_2\\ \tilde{\gamma}_1^T\frac{\partial v_4}{\partial z_3}\omega_1+\tilde{\gamma}_2^T\frac{\partial v_4}{\partial z_4}\omega_2\end{bmatrix} \quad (36)$$

Theorem: The proposed control (35a) ~ (35d) stabilizes the repulsive maglev suspension system (1) ~ (14) asymptotically if all the control gain k_i, i=1, 2, …, 6 in (28), (29), and (35a) are all positive.

Proof: If we define an adaptive Lyapunov function V:

$$V=\frac{1}{2}\begin{bmatrix}z_1 & z_2\end{bmatrix}\begin{bmatrix}z_1\\ z_2\end{bmatrix}+\frac{1}{2}\begin{bmatrix}z_3 & z_4\end{bmatrix}\begin{bmatrix}z_3\\ z_4\end{bmatrix}+\frac{1}{2}\begin{bmatrix}z_5 & z_6\end{bmatrix}\begin{bmatrix}z_5\\ z_6\end{bmatrix}$$
$$+\frac{1}{2}\tilde{\theta}_1^T\Gamma_1^{-1}\tilde{\theta}_1+\frac{1}{2}\tilde{\theta}_2^T\Gamma_2^{-1}\tilde{\theta}_2\geq 0 \quad (37)$$

By substituting equation (31) ~ (34), the time derivative of V becomes

$$\dot{V}=-k_1z_1^2-k_2z_2^2-k_3z_3^2-k_4z_4^2-k_5z_5^2-k_6z_6^2+z_3\tilde{\gamma}_1^T\omega_1+z_4\tilde{\gamma}_2^T\omega_2$$
$$-z_5\left(\tilde{\gamma}_1^T\frac{\partial v_3}{\partial z_3}\omega_1+\tilde{\gamma}_2^T\frac{\partial v_3}{\partial z_4}\omega_2\right)-z_6\left(\tilde{\gamma}_1^T\frac{\partial v_4}{\partial z_3}\omega_1+\tilde{\gamma}_2^T\frac{\partial v_4}{\partial z_4}\omega_2\right) \quad (38)$$
$$+\tilde{\gamma}_1^T\Gamma_1^{-1}\dot{\tilde{\gamma}}_1+\tilde{\gamma}_2^T\Gamma_2^{-1}\dot{\tilde{\gamma}}_2$$

Using the update law in equation (35c), (35d), one has

$$\dot{V}=-k_1z_1^2-k_2z_2^2-k_3z_3^2-k_4z_4^2-k_5z_5^2-k_6z_6^2\leq 0 \quad (39)$$

if k_i, i=1, 2, …, 6 are all positive. Finally, From LaSalle's Theorem [9], we obtain

$$\lim_{t\to\infty}z_1(t)=\lim_{t\to\infty}x_1(t)=0 \quad (40)$$

$$\lim_{t\to\infty}z_2(t)=\lim_{t\to\infty}x_2(t)=0 \quad (41)$$

The asymptotic stability of the maglev suspension system is thus achieved. □

5. Experimental Results and Discussion

5.1 Experimental Configuration

In this section, the maglev suspension system is studied experimentally to compare the performance of our robust adaptive backstepping controller with the results in [7], [8]. The maglev suspension system consists of the mechanism in Figure 1, a set of power amplifiers as actuators, Pentium 233 PC as the controller, inductive gauging sensors as feedback sources, a 12-bit AD converter and a 12-bit DA converter as system I/O devices. The resolution of sensors is 4μm with bandwidth of sensors is 3.3kHz. The control inputs are limited within ±9Volt to protect the stabilization coils. Due to the computational power of Pentium 233 PC, high-speed sampling is possible when complex control algorithm is implemented and the sampling error can be neglected. The block diagram for the proposed control algorithm is shown in Figure 5.

5.2 Experimental Results

The goals set for the maglev suspension system are the demonstration of stability, decoupling of the degrees of freedom, improvement of rail rigidity, and the robustness to system uncertainties. To make sure our controller can stabilize the maglev suspension system from its unstable nonlinear nature, the responses with respect to four different initial conditions A, B, C, D as indicated in Figure 6 should be tested. However, because of space limitation, only the results of cases A and C are shown. For comparison, an adaptive controller without backstepping [8] is also tested for the maglev system. Figures 7, 8, clearly show that the adaptive backstepping controller achieves superior performance over the adaptive controller without backstepping [8]. The settling time of the adaptive control is about 0.3 sec, and the settling time of our controller is 0.05 sec.

6. Conclusions

In this paper, we first introduce the classification of the maglev suspension systems, and clarify the working principles of our design, which is a repulsive maglev suspension system. Due to the lack of the information of magnetic parameters in our system, we transform the plant model into a parameterized form (21). By applying the adaptive backstepping control, the objective to asymptotically stabilize the system is achieved. The experiment results are also presented and compared with adaptive control without backstepping [8]. The results demonstrate that our adaptive backstepping control has better performance.

7. Acknowledgements

This work is supported by the National Science Council, Taiwan R. O. C. under project No. NSC87-2213-E-002-091.

8. Appendix

In equation (19), (20).

$$\alpha_1 = \frac{1}{I_2}\begin{bmatrix} I_{mA}\Omega_{ZA} + I_{mB}\Omega_{ZB} \\ I_{mC}\Omega_{ZC} + I_{mD}\Omega_{ZD} \end{bmatrix}_{2\times 1} \tag{42}$$

$$\alpha_2 = \frac{1}{M}\begin{bmatrix} I_{mA}\Omega_{ZA} + I_{mB}\Omega_{ZB} \\ I_{mC}\Omega_{ZC} + I_{mD}\Omega_{ZD} \end{bmatrix}_{2\times 1} \tag{43}$$

$$\beta_{11} = \frac{N_{SA}\Omega_{ZA} + N_{SB}\Omega_{ZB}}{I_z} \tag{44}$$

$$\beta_{12} = \frac{N_{SC}\Omega_{ZC} + N_{SD}\Omega_{ZD}}{I_z} \tag{45}$$

$$\beta_{21} = \frac{N_{SA}\Omega_{ZA} + N_{SB}\Omega_{ZB}}{M} \tag{46}$$

$$\beta_{22} = \frac{N_{SC}\Omega_{ZC} + N_{SD}\Omega_{ZD}}{M} \tag{47}$$

$$f_1 = \begin{bmatrix} (-a_1 + b_1 x_1)\frac{\mu_0}{2\pi}\left\{ -\frac{\left[e_M^2 - (c_M - a_1x_1 + x_2)^2\right]}{\left[(c_M - a_1x_1 + x_2)^2 + e_M^2\right]^2} + \frac{\left[e_M^2 - (-c_M - a_1x_1 + x_2)^2\right]}{\left[(-c_M - a_1x_1 + x_2)^2 + e_M^2\right]^2} \right\} \\ (a_2 + b_2 x_1)\frac{\mu_0}{2\pi}\left\{ -\frac{\left[e_M^2 - (c_M + a_2x_1 + x_2)^2\right]}{\left[(c_M + a_2x_1 + x_2)^2 + e_M^2\right]^2} + \frac{\left[e_M^2 - (-c_M + a_2x_1 + x_2)^2\right]}{\left[(-c_M + a_2x_1 + x_2)^2 + e_M^2\right]^2} \right\} \end{bmatrix}_{2\times 1} \tag{48}$$

$$f_2 = \begin{bmatrix} \frac{\mu_0}{2\pi}\left\{ -\frac{\left[e_M^2 - (c_M - a_1x_1 + x_2)^2\right]}{\left[(c_M - a_1x_1 + x_2)^2 + e_M^2\right]^2} + \frac{\left[e_M^2 - (-c_M - a_1x_1 + x_2)^2\right]}{\left[(-c_M - a_1x_1 + x_2)^2 + e_M^2\right]^2} \right\} \\ \frac{\mu_0}{2\pi}\left\{ -\frac{\left[e_M^2 - (c_M + a_2x_1 + x_2)^2\right]}{\left[(c_M + a_2x_1 + x_2)^2 + e_M^2\right]^2} + \frac{\left[e_M^2 - (-c_M + a_2x_1 + x_2)^2\right]}{\left[(-c_M + a_2x_1 + x_2)^2 + e_M^2\right]^2} \right\} \end{bmatrix}_{2\times 1} \tag{49}$$

$$g_{11} = (-a_1 + b_1 x_1)\frac{\mu_0}{2\pi}\left\{ \frac{-1}{\left[(d - a_1x_1 + x_2)^2\right]} + \frac{-1}{\left[(-d - a_1x_1 + x_2)^2\right]} \right\} \tag{50}$$

$$g_{12} = (a_2 + b_2 x_1)\frac{\mu_0}{2\pi}\left\{ \frac{-1}{\left[(d + a_2x_1 + x_2)^2\right]} + \frac{-1}{\left[(-d + a_2x_1 + x_2)^2\right]} \right\} \tag{51}$$

$$g_{21} = \frac{\mu_0}{2\pi}\left\{ \frac{-1}{\left[(d - a_1x_1 + x_2)^2\right]} + \frac{-1}{\left[(-d - a_1x_1 + x_2)^2\right]} \right\} \tag{52}$$

$$g_{22} = \frac{\mu_0}{2\pi}\left\{ \frac{-1}{\left[(d + a_2x_1 + x_2)^2\right]} + \frac{-1}{\left[(-d + a_2x_1 + x_2)^2\right]} \right\} \tag{53}$$

9. Reference

[1] P. K. Sinha, Electromagnetic Suspension, "Dynamics and Control". London. Peter Peregrinus, 1987.

[2] D. Cho, Y. Kato, and D. Spilman, "Sliding Mode and Classical Control of Magnetic Levitation Systems". IEEE Control Syst. Mag., vol. 13,no. 1, pp. 42-48, 1993.

[3] D. L. Atherton, "Maglev using paermagnets", IEEE Trans. Magn., vol. 16,no. 1., pp. 146-148, 1980.

[4] M. Morishita, T. Azukizawa, S. Kanda, N. Tamura, and T. Yokoyama, "A new maglev system for magnetically levitated carrier system", 1986 Int. Conf. Maglev and Linear Drives, Vancouver, B. C., May 1986.

[5] O. Tsukamoto, K. Yasuda, and J. Z. Chen, " A New Magnetic Levitation System with ac Magnets", IEEE Trans. Magn., vol. 24, no. 2, pp. 1497-1500, 1988.

[6] R. Williams, J. R. Matey, Y. Arie, and J. Rathee, "The effect of mass and pole strength on the levitation height of the magnet over a superconductor", J. App. Phys., vol. 65, no. 9, pp. 3583-3585, 1989.

[7] I.Y. Wang. A Magnetic Levitation Silicon Wafer Transport System. Ph.D. Thesis, The University of Texas at Austin, 1993.

[8] K. N. Wu, and L. L. Chen, "Adaptive control of a four-track maglev system", Journal of Control Systems and Technology 4, 4,pp. 295-302, 1996.

[9] Krstic, Kanellakopouslos, and Kokotovi'c, "Nonlinear and Adaptive Control Design", Wiley Interscience, 1995.

[10] E. M. Purcell, Electricity and Magnetism, Berkeley Physics Course vol 2. McGraw-Hill, 1965.

[11] J. G. David, Introduction to Electrodynamics, Prentice-Hall, Inc., Englewood Cliffs, New Jersey, 1981.

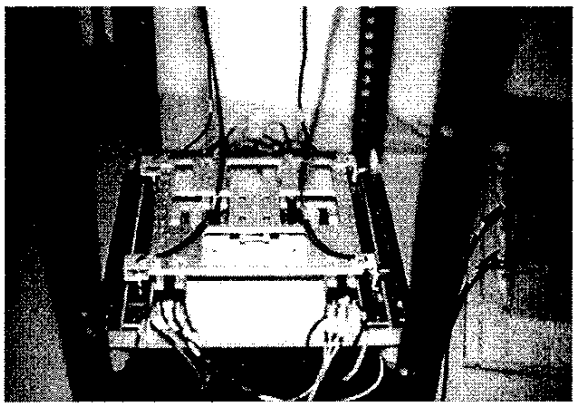

Figure 1. Photograph of the physical system

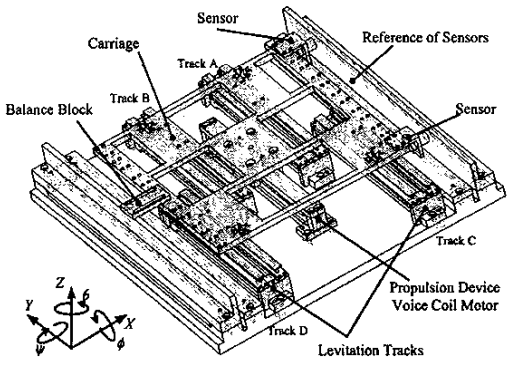

Figure 2. A 3-D view of a section of the entire system.

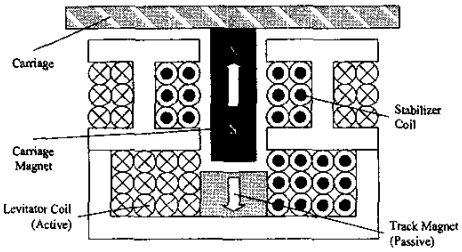

Figure 3. The cross-section of levitation track.

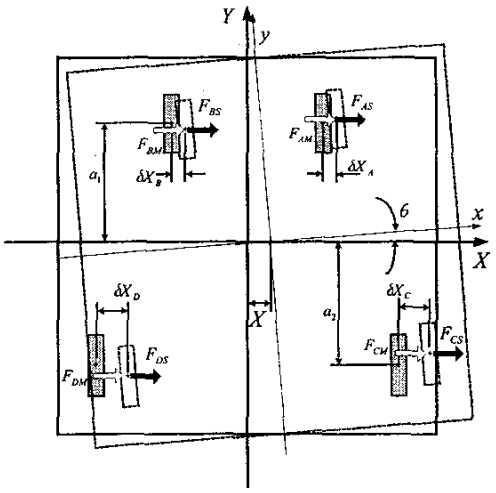

Figure 4. The free body diagram of the carriage after undergoing X translation and θ rotation.

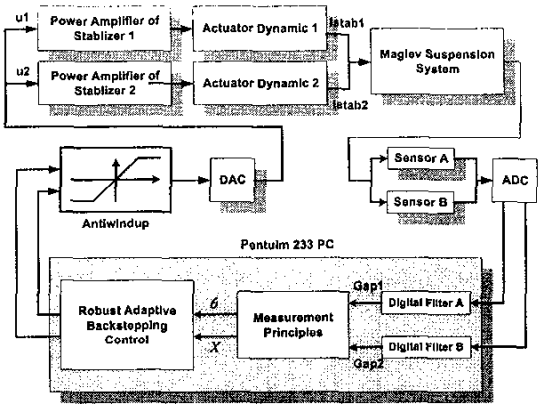

Figure 5. Block diagram of the closed loop system.

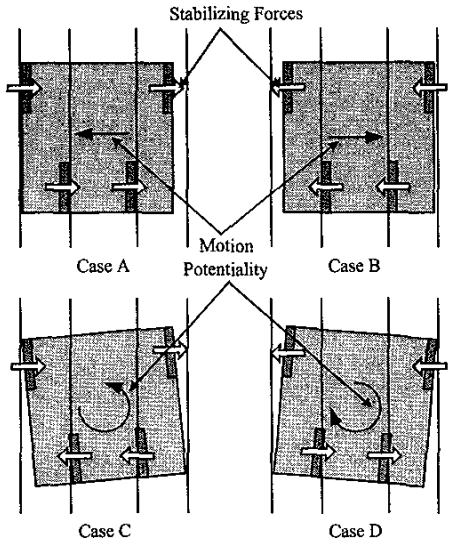

Figure 6. Four typical cases of initial condition (IC). Where Case A is the maximum positive translation IC, Case B is the maximum negative translation IC, Case C is the maximum positive rotation IC, and Case D is the maximum negative rotation IC.

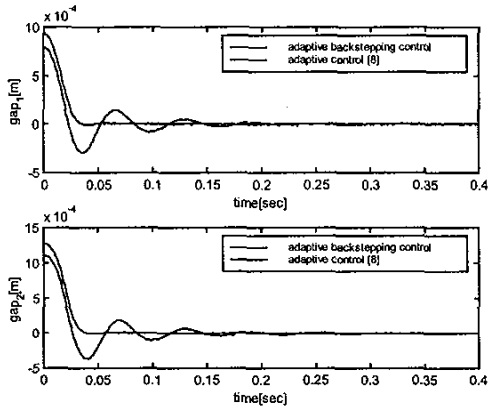

Figure 7. Experiment result of initial condition Case A.

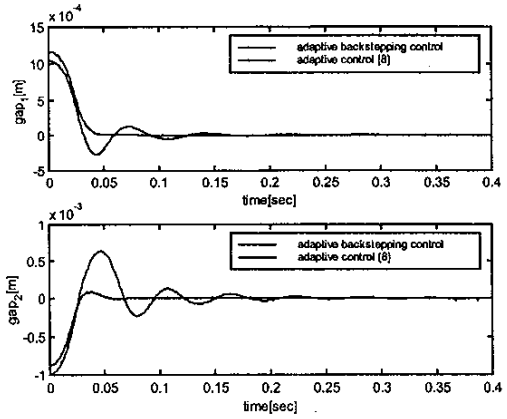

Figure 8. Experiment result of initial condition Case A.

Table 1.

	Active Levitator	Stabilizer
Track A	I_{lev1}	I_{stab1}
Track B	I_{lev1}	I_{stab1}
Track C	I_{lev2}	I_{stab2}
Track D	I_{lev3}	I_{stab2}

Table 2. Parameters list of the model

-Mass of the Carriage M	648.812g
-Momentum Inertia J_Z	5.47172×10^6 g · mm^2
-Dimension Parameter a_1	64mm
-Dimension Parameter a_2	64mm
-Dimension Parameter b_1	40mm
-Dimension Parameter b_2	80mm
-Dimension Parameter d	6.5mm
-Dimension Parameter c_M	4mm
-Dimension Parameter e_M	15mm
-Coils NO. of Stabilizer A N_{SA}	60turns
-Coils NO. of Stabilizer B N_{SB}	60turns
-Coils NO. of Stabilizer C N_{SC}	60turns
-Coils NO. of Stabilizer D N_{SD}	60turns
-Dipole Moment of Carriage Magnets A Ω_{ZA}	3.74Am^2
-Dipole Moment of Carriage Magnets B Ω_{ZB}	3.74Am^2
-Dipole Moment of Carriage Magnets C Ω_{ZC}	3.74Am^2
-Dipole Moment of Carriage Magnets D Ω_{ZD}	3.74Am^2
-Magnetization Current of Track Magnet A I_{mA}	5.14.8126A
-Magnetization Current of Track Magnet B I_{mB}	5.14.8126A
-Magnetization Current of Track Magnet C I_{mC}	5.14.8126A
-Magnetization Current of Track Magnet D I_{mD}	5.14.8126A